

# Semiannual Variation at the Base of the Thermosphere

ADAM KOCHANSKI—*Air Resources Laboratories, Environmental Research Laboratories,  
NOAA, Silver Spring, Md.*

**ABSTRACT**—In the 80- to 105-km height region, zonal winds and their vertical shears, as well as ionospheric drifts, show a semiannual variation that is in phase with a similar oscillation in temperature and density at satellite heights (190–1130 km). At higher latitudes, the effect is purely semiannual, but at 35° latitude a 12-mo term seems to be superimposed. Similar variations must exist in the latitudinal temperature gradient that is associated with vertical shears. Temperature data were not available for this study, requiring a chain of assumptions in order to draw some inferences regarding this parameter. Under these assumptions, the mean temperature of the 80- to 105-km layer could possess temporal variations nearly parallel to changes observed in shears. This would suggest,

for midlatitudes, a temperature variation composed of a 12-mo and a 6-mo term of roughly equal magnitudes. Such variations in temperature and in the latitudinal temperature gradient could be explained by systematic changes in the vertical thermal structure of the 80- to 105-km layer.

At least in the parameters of motion, a latitudinal effect appears to be present up to a height of 160 km, whereas seasonal changes attenuate rapidly above 100 km. It is thus possible that the semiannual variation in motion parameters is exposed, as a primary factor, at heights not far removed from 120 km. Whether an analogous situation exists in temperature is at present a matter of conjecture.

## 1. GENERAL CONSIDERATIONS

One of the outstanding characteristics of the upper atmosphere is the semiannual density variation. Discovered by Paetzold and Zschörner (1960, 1961) from satellite drag observations at heights from 210 to 650 km, it was described in detail by Jacchia et al. (1969) for five heights between 250 and 656 km. The same variation was found at 1130 km (Cook and Scott 1966) and at 190 km (King-Hele and Hingston 1968). The curve of this oscillation is slightly asymmetrical in shape as if it contained a semiannual and an annual term, but since both terms depend in the same way on the 10.7-cm solar flux, Jacchia (1965) concluded that these are not separate phenomena, but are inherent features of a single variation. The primary maximum of this variation appears in late October, the secondary one in early April. The primary minimum is in July, the secondary one in January. However, in individual years the times of maxima and minima can vary by over 1 mo. Similarly, in some years, the April maximum may be equal in magnitude to the October maximum. The variation appears to be independent of latitude and, in all cases, its phase is constant with height.

According to Jacchia (1965), the direct cause of the semiannual density variation is a parallel variation of temperature in the thermosphere. However, temperature variations for the diffusion model assumed by Jacchia were inadequate to explain the large amplitude of the semiannual density variation near 1100 km and as an additional cause, Cook (1967, 1968) suggested a variation in the height of the helium turbopause. In general, changes of the diffusive equilibrium level (105–120 km) would explain the enhanced semiannual effect at 1100 and 190 km. Cook (1969) has also suggested a global semi-

annual density variation at 90 km with maxima in April and October; this could give rise to a semiannual density effect at heights up to 200 km without the necessity of postulating large temperature changes near 120 km.

Becker (1966) has found a similar semiannual variation in the height of the peak of the F2 region at Lindau, Germany (51°N, 10°E), with dates of the maxima, however, departing in some years as much as 2 mo. from those for exospheric temperatures. Also, the evening–morning differences of the height of the sodium layer near 90 km show a regular semiannual variation (Sullivan and Roberts 1968) with maxima occurring near the equinoxes corrected for atmospheric screening; that is, around February 22 and October 21. Elford and Roper (1967) noted a pronounced semiannual variation near 91 km in the rate of exchange of turbulent energy and in the kinetic energy of the diurnal tide, and suggested that the height of the turbopause may possess a similar variation.

For the lower regions (20–60 km), Angell and Korshover (1970) indicated that the amplitude of the semiannual temperature variation grows with latitude and elevation, exceeding at 60 km the values of 3°K at 30°N, and 4°K at 64°N. The first maximum of this variation generally occurs in May. Monthly temperature curves from the COSPAR International Standard Atmosphere (CIRA, COSPAR Working Group IV 1965) suggest that a pronounced semiannual variation should appear in latitudes 0°–35° at 60 km and nearly vanish at 80 km. The first maximum of this variation would also be in May. Cole (1968) found a strong 6-mo harmonic in density in the 45- to 70-km region at lower latitudes, agreeing in phase with the CIRA density model. Unfortunately, Cole's data did not extend beyond latitude 32°N. In the stratosphere, the semiannual effect in lower latitudes is usually attributed to the double passage of the sun over the Equator and

TABLE 1.—Stations and length of record used in the analysis of winds and ionospheric drifts

Station	Lat.	Long.	Record for $\bar{u}$	Record for $\Delta\bar{u}/\Delta z$
Adelaide	35°S	138°E	Dec. 1960–Dec. 1961	same as $\bar{u}$
Jodrell Bank	53°N	2°W	Sept. 1953–Dec. 1958	1954–55
Kühlungsborn	54°N	12°E	Jan. 1962–Dec. 1965	none
Birdlings Flat	44°S	173°E	Parts of 1964, 66, 67	same as $\bar{u}$

heating by ozone absorption, but its growth in high latitudes remains unexplained. Perhaps the most important common feature of the semiannual variation in density and temperature in the mesosphere and at heights over 190 km is phase similarity.

The ultimate origin of the semiannual density and temperature variation in the thermosphere is not yet understood. The solar wind theory (Paetzold and Zschörner 1961) is considered untenable under closer scrutiny. A purely terrestrial cause was suggested by Johnson (1964) who postulated a meridional circulation at ionospheric levels to compensate for a latitudinal asymmetry in heating of the thermosphere by solar ultraviolet radiation. In general, the heat transfer from the upper atmosphere to the mesopause would produce a relatively warm thermosphere near the equinoxes and a cold one near the solstices. Interestingly, near the height of 140 km this mechanism would require meridional components of only 7–10 m/s. Since vertical compensation is involved, pressures and temperatures in the upper mesosphere should still be affected by this mechanism.

The present paper attempts to analyze the semiannual and annual effect in the 80- to 105-km region. Lacking coherent temperature series, the analysis was concentrated on the prevailing wind and its vertical shears. Temperature estimates were obtained by assuming certain variations at the 80-km level and considering advective changes in the 80- to 105-km layer shown by wind data. Four basic sources of information were utilized (table 1). The most detailed one concerned meteor winds from Adelaide, Australia, available for 2-km levels within the height range of 75–105 km (Roper and Elford 1965). Meteor winds from Jodrell Bank, England, were also used (Greenhow and Neufeld 1961). In addition, ionospheric drift data were employed; drifts from Birdlings Flat, New Zealand, were available for seven levels within the 80- to 104-km layer, and drifts from Kühlungsborn, Germany, for the heights near 95 km (Sprenger and Schminder 1967). Drift data were utilized on the basis of recent evidence (Fraser and Kochanski 1970) that seasonal and monthly averages of ionospheric drifts and neutral winds yield very similar results.

Conventions used throughout the text are listed below. An east to west wind is defined as *easterly* and labeled E on the diagrams, a south to north wind is *southerly*. The magnitude of the wind vector is  $|\mathbf{V}| = (u^2 + v^2)^{1/2}$  where  $u$  and  $v$  are zonal and meridional components, respectively. According to the thermal wind equation, an easterly vertical shear (also labeled E on the diagrams) is positive and indicates presence of warmer air in the poleward direction.

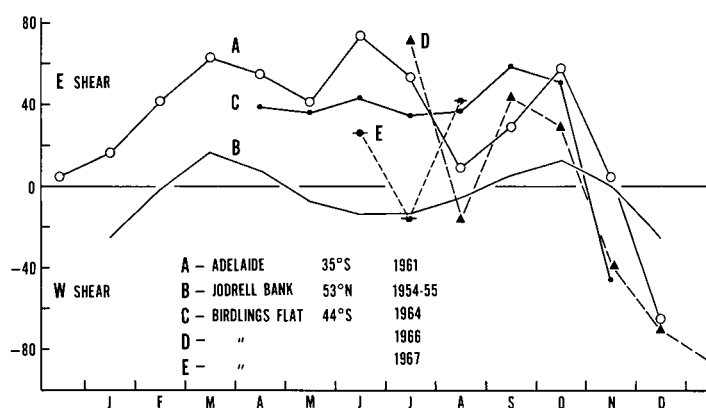


FIGURE 1.—Observed 79- to 103-km shears [ $\text{m}\cdot\text{s}^{-1}\cdot(24\text{ km})^{-1}$ ] of the zonal wind component. Curves for Adelaide and Jodrell Bank are based on meteor winds, those for Birdlings Flat on ionospheric drifts. All data are plotted in real time; that is, without reversing months for curves from Northern and Southern Hemispheres.

A westerly shear (symbol W) suggests colder air toward the pole. The abbreviation, "U.S. Standard," is used in the text when referring to the U.S. Standard Atmosphere Supplements 1966 (COESA 1966).

## 2. SEMIANNUAL VARIATION IN ZONAL WINDS AND SHEARS

The base of the thermosphere (80–105 km) encompasses several subregions with radically different shear and temperature characteristics. For these subregions, shear data show seemingly disorganized variations, but a much clearer picture emerges when the total shear is analyzed. It is likely that in this highly transitional zone some properties are brought to light only when overall conditions of a deep layer are considered. Thus, whenever possible, this zone, 25 km in thickness, will be treated as an entity.

The observed 79- to 103-km shears of the zonal component of the prevailing wind are shown in figure 1. Curves A and B are based on meteor winds; curves C, D, and E, on ionospheric drifts. The data for the Northern and Southern Hemisphere are plotted in real time; that is, without reversing the seasons. The most regular semiannual variation is seen at Jodrell Bank (curve B). At latitudes 35°S and 44°S, there are still two maxima near the equinoxes, with a third maximum appearing in June or July; a well-delineated primary minimum (maximum westerly shear) is seen in December or January. The shape of curve A, and to some extent of C and D, suggests

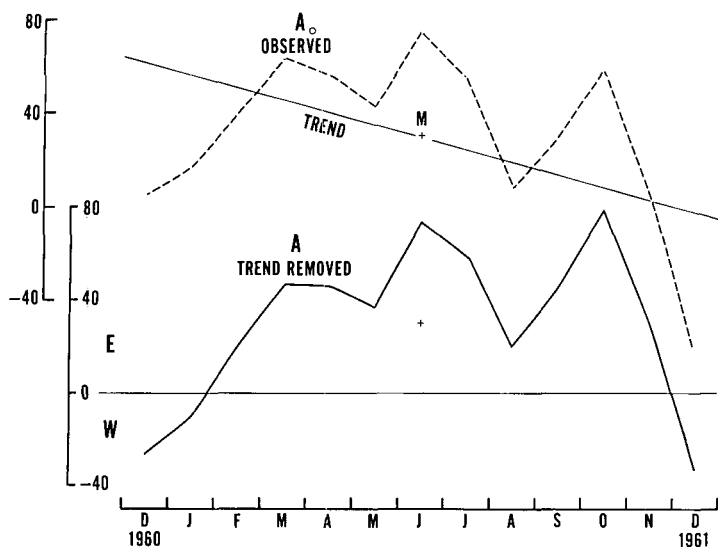


FIGURE 2.—Long-term trend assumed to be present in Adelaide shears. Curve  $A_0$  is based on observed values, while curve A represents a seminormalized version. Shear units are  $[m \cdot s^{-1} \cdot (24k m)^{-1}]$ .

that in addition to the semiannual effect an appreciable 12-mo term may be present. There is a good deal of similarity among the four curves from the Southern Hemisphere except that some phase shifts occur in the positions of maxima and minima. Quite likely, these curves contain effects of year-to-year variability and data uncertainties that tend to mask basic variations.

A clear case of a 13-mo trend is seen in Adelaide shears (curve  $A_0$ , fig. 2) when values for December 1960 and December 1961 are compared. For further considerations it was thought desirable to remove this trend by applying a least-squares fit to  $A_0$  (slant line). The trend-removed values are represented by curve A, which can be considered a seminormalized version of  $A_0$ . Note that the primary maximum in curve A then appears in October, but that the high peak in June remains unchanged.

Figure 3 introduces further evidence regarding the semiannual variation at meteor heights. Apparently this variation is present not only in the shears but also in the zonal component itself in both meteor winds and ionospheric drifts. Figure 3A compares zonal shears from the 79–103 km layer with the semiannual variation of exospheric temperatures (curve J). Curve a represents trend-removed shears from Adelaide for 1961, curve b depicts 1954–55 shears from Jodrell Bank, and J was taken from Jacchia et al. (1969). Curves b and J are quite similar, while the peak in the middle of curve a suggests that another oscillation is imposed on the semiannual effect. Figure 3B shows zonal components of the prevailing wind and ionospheric drifts. Curve c is for Jodrell Bank and applies to 92 km, but presumably includes data from the whole range of the meteor regime. Curve d is for Adelaide and applies to a thin layer from lower heights, but it is the best choice from several tests; this height restriction suggests that the layer in which a clear semiannual variation appears may have a latitudinally dependent slope. Two points are shown for August (for

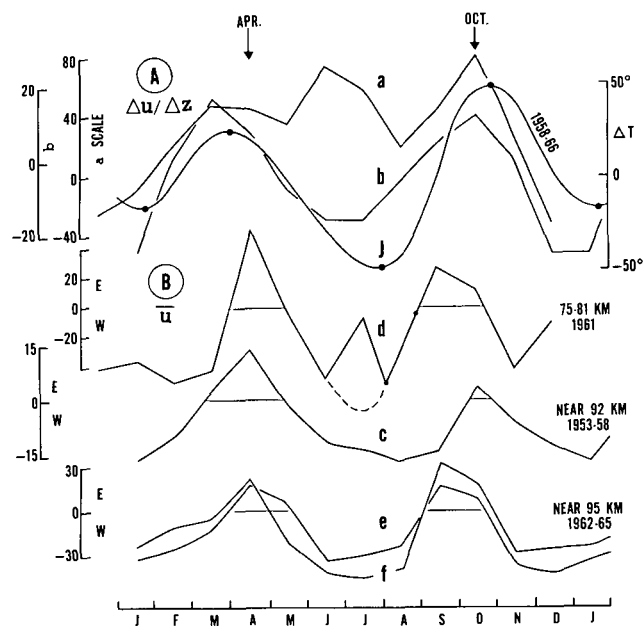


FIGURE 3.—(A) variations in shear  $[m \cdot s^{-1} \cdot (24 km)^{-1}]$  compared with the semiannual variation of exospheric temperatures ( $^{\circ}K$ ) from Jacchia et al. (1969) represented by curve J. (B) shows zonal components (m/s) of meteor winds (curves d and c) and ionospheric drifts (e and f). All data are plotted in real time.

observational periods of August 1–6 and 17–24) to illustrate the unrepresentativeness of short period means as monthly averages. In connection with curve d of figure 3B, it should be mentioned that just below meteor heights a phase shift of  $180^{\circ}$  probably occurs in the semiannual variation of zonal winds. Reed (1966) has shown that, at latitudes  $22^{\circ}N$  and  $8^{\circ}S$  in the 15- to 64-km region, maxima of *westerlies* occur in April and October. The amplitude of this 6-mo harmonic is considerable at  $8^{\circ}S$  but decreases at  $22^{\circ}N$ .

In figure 3, curves e and f show zonal components of ionospheric drifts at the height of about 95 km at K hlungsborn; they represent 1962–65 averages and apply to measurements at the frequencies of 185 and 245 kHz. Evident in e and f is a surprisingly regular semiannual effect with the fall maximum, however, occurring in September rather than in October.

The semiannual variation appears also in the 245- to 185-kHz drift differences, as if these differences represented a vertical shear. While the reflection heights for these two frequencies cannot be known exactly even to the experimenters, it is likely that the 245-kHz data came from greater heights. These differences in the zonal component of drifts are shown in figure 4. The magnitude of the variations is somewhat smaller than in the Adelaide shears but greater than at Jodrell Bank. We do not suggest, however, that K hlungsborn readings were separated by a height interval of as much as 24 km, and this point must at present remain unexplained.

For Jodrell Bank and K hlungsborn, the behavior of the semiannual variation in individual years could be examined. Some phase distortion was noted, but this may be due to the insufficient data on which monthly means were based and to masking effects of other variations.

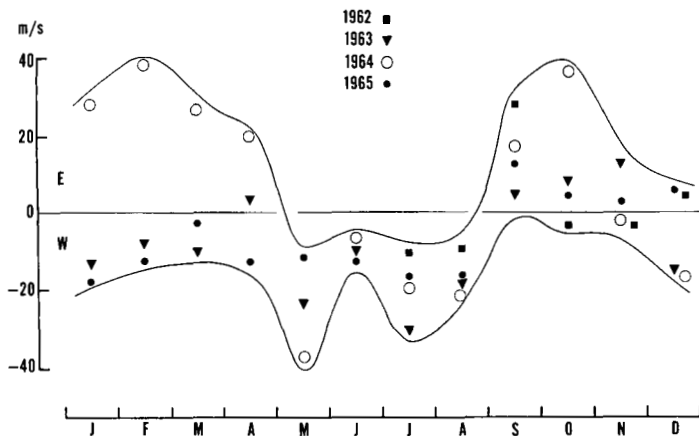


FIGURE 4.—Differences between ionospheric drift measurements at 245 kHz and 185 kHz [i.e.,  $u(245 \text{ kHz}) - u(185 \text{ kHz})$ ] for Kühlungsborn. Values were derived from monthly means of zonal components. Note that the first half of the 1962 data is missing.

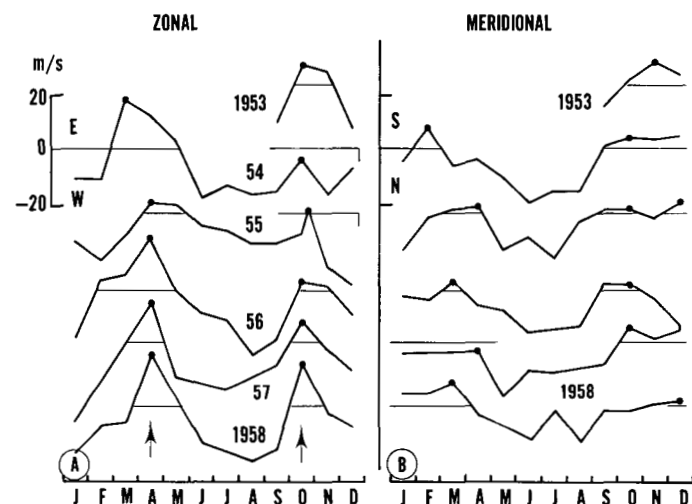


FIGURE 5.—Semiannual variation in (A) zonal and (B) meridional meteor winds at Jodrell Bank ( $53^\circ\text{N}$ ) at approximately 92 km. Adapted from Greenhow and Neufeld (1961).

Figure 5A shows the zonal component at Jodrell Bank; the fall maximum appears always in October but its magnitude is smaller than that of the April maximum. Figure 5B shows a rather ill-defined semiannual effect in the meridional component. This component is weaker than the zonal wind, suggesting that latitudinal rather than longitudinal changes of temperature and pressure are of prime importance at these heights.

Figure 6 shows zonal components from ionospheric drift measurements at Kühlungsborn. While the spring maximum occurs always in April, the fall maximum appears mostly in September, and in only three cases out of seven is the fall maximum a dominant one. Whether such shifts in phase and in relative magnitude of maxima are real or merely an effect of sampling and reduction technique could not be ascertained without additional basic data.

The uncertainties concerning semiannual variation in individual years were especially evident in the case of the Adelaide series for 1961. By choosing to analyze the

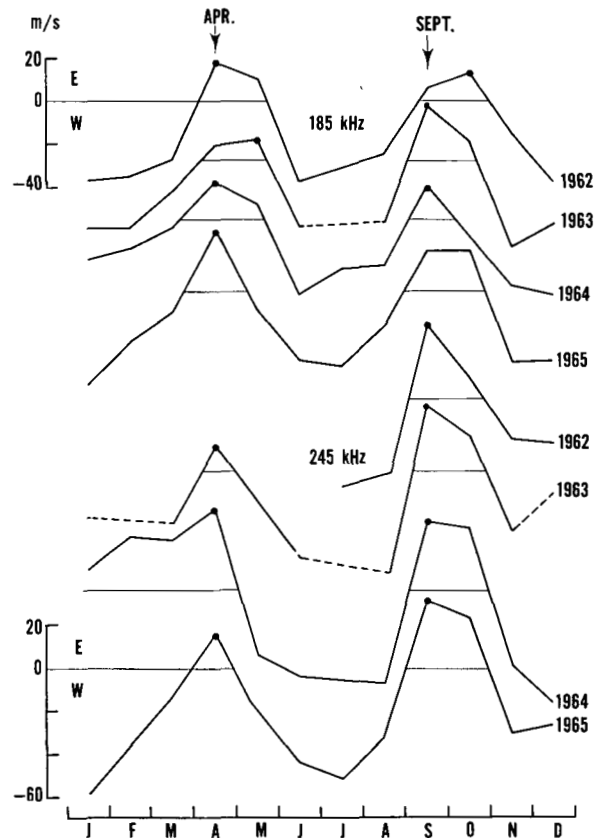


FIGURE 6.—Semiannual variation in the zonal component of ionospheric drifts at about 95 km over Kühlungsborn ( $54^\circ\text{N}$ ). Data were adapted from Sprenger and Schminder (1967).

79- to 103-km shear we have risked dealing with values bearing very large errors that, due to the fitting technique used (Groves 1959), occur at the boundaries of meteor wind observations; that is, at 75 and 105 km. Because the total shear of the 79- to 103-km layer is simply a difference of zonal components at these two levels divided by the height interval, errors in the defining values undoubtedly concealed the true shear values and, as far as semiannual effect is concerned, the real variation. Adelaide data suggested that the strongest zonal components and largest shears appear at either 75 or 105 km. While for the 105-km level this is supported by sodium cloud observations, there is no justification for maxima of  $\bar{u}$  and shear at 75 km. Furthermore, physically improbable boundary means appeared in April and October [ $\bar{u}=211 \text{ m/s}$ ,  $\bar{v}=113 \text{ m/s}$ , and  $\Delta u/\Delta z=111 \text{ m}\cdot\text{s}^{-1}\cdot(2 \text{ km})^{-1}$ ]. But these 2 mo also carried the largest boundary errors in the whole series, exceeding those for other months by a factor of three. Consequently, the zonal components near the boundaries for October were adjusted by 50 percent of the root-mean-square (rms) error, and those for April by 150 percent. Adelaide shears shown in figures 1 and 2 were based on these adjusted values.

### 3. DEDUCED SYSTEMS OF GENERAL CIRCULATION

An important feature of wind and shear distribution at Adelaide is that it describes qualitatively otherwise known details of circumpolar circulation and accompanying

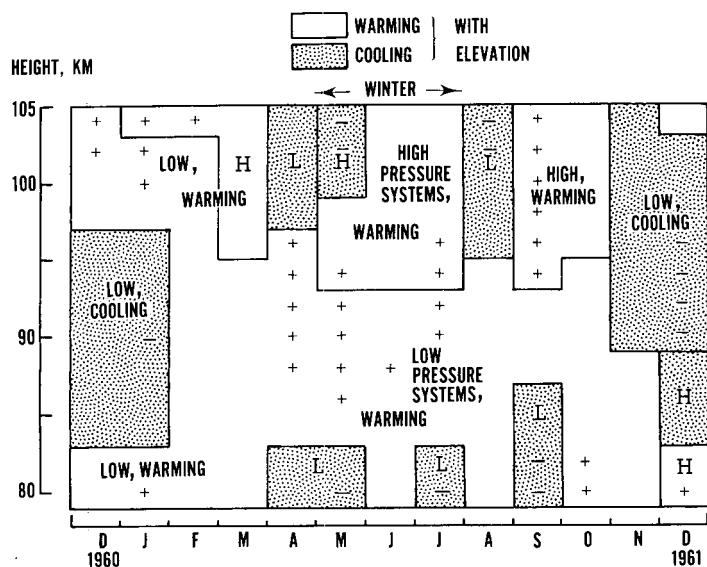


FIGURE 7.—Pressure systems south of Adelaide and their warming or cooling with elevation, as deduced from the prevailing wind and shears. Symbols + and - indicate especially large amounts of warming or cooling in 2-km strata.

seasonal variations of temperature. If tentative synoptic maps at 80 km (Warnecke and Nordberg 1965) are correct, circumpolar systems do extend to low latitudes with monotonic changes in pressure and thermal structure. Thus, inferences from Adelaide data, using the thermal wind equation, may be valid to high latitudes providing nonlinear effects are not too large. By combining the vectors of prevailing wind and shear, we deduced pressure systems located in the general poleward direction with respect to Adelaide, and whether they warmed or cooled with elevation. The assumption is that the systems are circular in shape.

The results are shown in figure 7, which is based on data in 2-km steps. Blank areas indicate warming with elevation, shaded areas denote cooling. Layers with largest warming and cooling (26 percent of total cases), are marked with plus and minus symbols. Labels "High" or "H" stand for high pressure systems, and "Low" or "L" for low pressures. The directional location of the centers of these systems with respect to Adelaide is not shown, but the count indicates that 72 percent of the centers were located in the southwest to southeast quadrant, versus 50 percent expected from random probability; a still higher ratio applies to the sector south-southwest to south-southeast that contains 40 percent of the centers, versus 25 percent expected. This grouping strongly suggests that Adelaide data reflect systems centered near the pole.

Figure 7 is then compared with the existing ideas of circumpolar circulation, which above 80 km are conceptual rather than based on observations. It is known that in winter the circumpolar cyclonic vortex extends through the whole mesosphere; at still higher elevations this vortex presumably fills up and changes into a warm anticyclone. The warming is probably due to descending motions and to the recombination of atomic oxygen (Kellogg 1961). The

TABLE 2.—Harmonic terms of 79- to 103-km shears of the zonal wind component at Adelaide based on trend-removed values for 1961

Period	Amplitude	Phase (Jan 15=1.0)
(mo)	(m/s)	(mo)
12	26.9	6.7
6	19.2	3.9
4	25.6	2.3
3	9.6	3.8
2.4	3.6	1.3

May through July (fig. 7) pressure pattern closely resembles this conceptual model. Remnants of the cold vortex are seen near 80 km; then the vortex becomes warmer with height and changes into a warm anticyclone. In summer, a vast anticyclonic vortex is known to exist through the mesosphere with a compensatory cyclonic system presumably developing at still greater heights. Figure 7 shows such cold cyclonic circulation in several months of the Southern Hemisphere summer; however, the warm mesospheric anticyclone is probably at heights below 80 km as shown in December 1961. In addition, figure 7 reveals several hitherto unknown features. Equinoctial months (March, September, October) show a warm anticyclone in the uppermost layers, similar to that during southern winter. April and August, on the other hand, indicate cooling at the highest levels. Thus, while figure 7 agrees with otherwise known summer-winter circulation changes, it also reveals distinct equinoctial features at heights over 95 km.

#### 4. SEMIANNUAL AND ANNUAL COMPONENT IN ADELAIDE SHEARS

While the semiannual effect dominates shear variations at Jodrell Bank, it is undoubtedly present also at lower latitudes where it coexists with a seasonal term. It can be demonstrated that Adelaide shears may be interpreted as the sum of a 6- and a 12-mo variation of roughly equal amplitudes.

The results of harmonic analysis were somewhat ambiguous in this case (table 2), showing a strong 4-mo term that has no known physical explanation. On the other hand, the phases of the second, third, and fourth harmonics were similar and close to the phase of the semiannual temperature oscillation in the thermosphere. If, as suggested later, the variations of shear and temperature in the 80- to 105-km layer are nearly parallel, terms resembling temperature oscillations should be adequate to describe shear data. Hence, Adelaide shears were compared with a series of synthetic curves that were built using only a 6-mo and a 12-mo term. The 6-mo term,  $J'$ , had at all times the phase and shape of the exospheric temperature variation in 1961, as given by Jacchia et al. (1969). The 12-mo term generally resembled the temperature variation in the 80- to 105-km layer from the U.S. Standard, but its phase was allowed to vary by half a month and its amplitude by a factor of 0.5–1.5 with respect to the amplitude of  $J'$ .

Examples are shown in figure 8 where A represents Adelaide shears while B, C, and D are synthetic curves. The correlation coefficients between A and B, C, and D

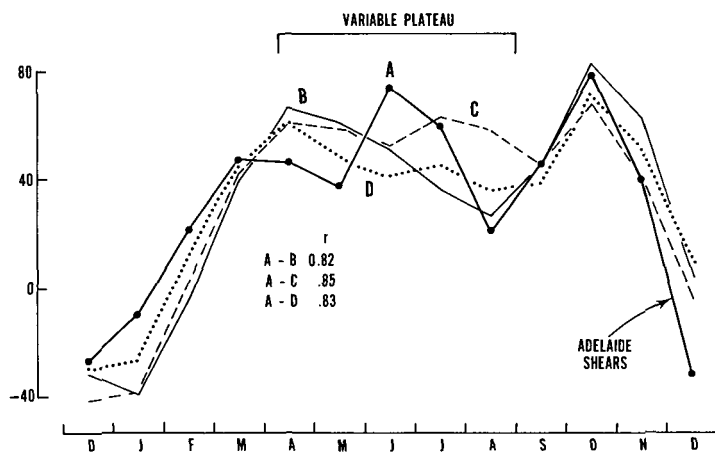


FIGURE 8.—Adelaide shears (curve A) compared with synthetic curves B, C, and D. Composite curves contain a 6-mo term with the shape and phase of the semiannual variation in exospheric temperatures in 1961 and a varying 12-mo term. Units:  $\text{m} \cdot \text{s}^{-1} \cdot (24 \text{ km})^{-1}$ .

are 0.82, 0.85, and 0.83 respectively; for the 90-percent confidence limit, the true coefficients would be within the 0.67–0.93 range. The outstanding feature of the synthetic curves is an ill-defined plateau from April to August with easily changeable details. In contrast, the primary minimum (maximum westerly shear) that occurs during southern summer and the October maximum are always clearly defined. Noteworthy in curve C are three maxima analogous to those in curve A. The flat plateau with changeable details was also seen in the Birdlings Flat data (see fig. 1). Of interest in figure 8 is the ratio of October maximum to April maximum: in Jacchia's curve this ratio is 1.33 while for curves B, C, and D it is 1.46, 1.24, and 1.29, respectively. These and other similarities do not seem coincidental and suggest that Adelaide shears contain, in addition to a 12-mo variation, a strong semiannual component.

In the synthetic curves of figure 8, the maximum of the 12-mo term is always in July. For curve B, this term is sinusoidal and the amplitude equal to that of  $J'$ . In C and D, the 12-mo term is nonsymmetrical and conforms in shape to the temperature curve at 80 km and  $35^\circ$  latitude, as given by CIRA. For C and D, the amplitude of this term is 1.25 and 1.0 in ratio to  $J'$ . In all examples, the comparison of A with the fitting curves leaves small residuals that exhibit a clear 3- to 4-mo periodicity.

## 5. ANALOGY TO VARIATIONS OF MESOSPHERIC TEMPERATURES

A thorough investigation of temperature variations in the 80- to 105-km region is at present impossible because of insufficient data. An important possibility is suggested, however, by analogy to the mesosphere. According to the CIRA model (which supplies monthly values up to 80 km), a semiannual variation in temperatures at low latitudes is reflected in the horizontal temperature gradient over a very wide latitude range.

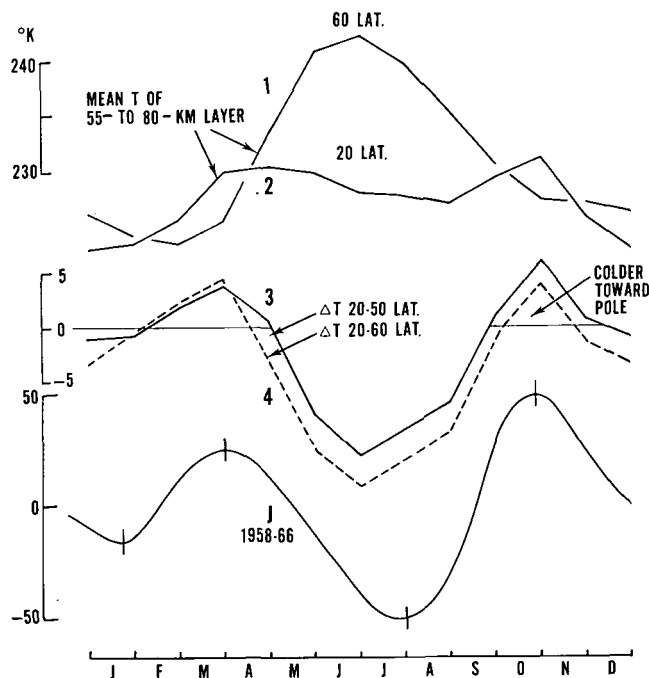


FIGURE 9.—Variations in mean mesospheric temperatures (curves 1 and 2) and in latitudinal temperature differences (curves 3 and 4), compared with the semiannual variation in exospheric temperatures (curve J). Mesospheric data from CIRA are plotted for the Southern Hemisphere.

For low latitudes, CIRA indicates a pronounced semiannual temperature variation up to about 75 km. At latitudes greater than  $40^\circ$ , a 12-mo variation is dominant at all heights. This behavior is reflected in the mean temperatures of the 55- to 80-km layer, as indicated by curves 1 and 2 of figure 9. Curves 3 and 4 show latitudinal temperature differences,  $\Delta T$ , and are compared with curve J representing the variation in exospheric temperatures taken from Jacchia et al. (1969). For the Northern Hemisphere, curve 1 is reversed, but the  $\Delta T$  curves remain similar to those shown in figure 9. Apparently, the 55- to 80-km layer normally exhibits a semiannual variation in  $\Delta T$  despite the fact that the temperatures at higher latitudes possess a dominant 12-mo oscillation. Considering thermal compensation between the lower mesosphere and lower thermosphere (as is inherent in the U.S. Standard and CIRA models), we may assume that an analogous situation is created in the 80- to 105-km layer but with signs of  $\Delta T$  the reverse of those shown in figure 9. This would produce a clear semiannual shear variation much like that at Jodrell Bank without requiring presence of a strong semiannual variation in temperature at high latitudes. Although this point was not adopted in the following sections, it offers an alternative to our estimated temperature variations at  $60^\circ$  latitude (cf. fig. 13).

## 6. HYPOTHESIS OF TEMPERATURE VARIATIONS

It has been shown in previous analyses that, in the 80- to 105-km layer at both low and high latitudes, a semiannual effect is present in the zonal wind, its vertical

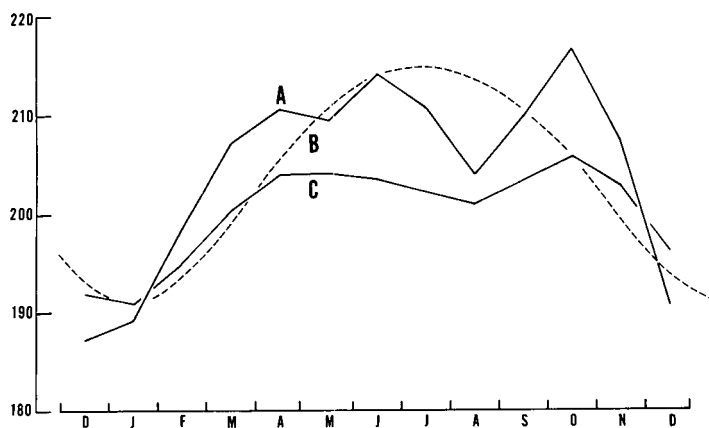


FIGURE 10.—Inferred mean temperatures ( $^{\circ}\text{K}$ ) of the 80- to 104-km layer at Adelaide (curve A) compared with  $\bar{T}$  suggested by the U.S. Standard for  $30^{\circ}$  latitude (curve B). Line C shows temperatures at the 80-km level used in computations of A.

derivative, and in the horizontal derivative of temperature. It is a matter of conjecture whether the semiannual effect appears also in temperature, but as a working hypothesis we shall assume that it does.

At least for Adelaide and Jodrell Bank, the data indicate that the total 80- to 105-km easterly shear is correlated with warm advection and the westerly shear, with cold advection. A stage with a zero advection also exists in some months (i.e.  $\Delta u/\Delta z \approx 0$ ), corresponding to  $T_{80\text{ km}} \approx \bar{T}_{80-105\text{ km}}$  according to the U.S. Standard. This implies that in situ temperatures of the 80- to 105-km layer are higher than those at 80 km in case of easterly shear, and lower for westerly shear. It is then possible to deduce in situ temperatures from shear data, using the technique described in the appendix.

The inferred mean temperatures of the 80- to 104-km layer for Adelaide are shown in figure 10 by curve A. They are compared with purely seasonal temperature variations suggested by the U.S. Standard (curve B). The latter was shifted upward by  $9^{\circ}\text{K}$  so that its mean coincides with that of curve A. Line C shows the assumed temperatures at the 80-km level necessary to compute A. Line C is the sum of (1) Jacchia's exospheric temperature variation for 1961 with the range (hereafter called "amplitude") scaled down to  $13^{\circ}\text{K}$  (i.e., to one-tenth of its original value) and (2) a sinusoidal 12-mo term with maximum in July and an amplitude of  $15^{\circ}\text{K}$ . The amplitude of term (2) was chosen to be close to the annual amplitude of  $13^{\circ}\text{K}$  suggested by the U.S. Standard for  $30^{\circ}$  latitude and 78- to 82-km heights. Then two conditions were imposed in choosing the amplitude of term (1): that it should satisfy a reasonable extrapolation, from 60 to 80 km, of the amplitude of semiannual temperature variation given by Angell and Korshover (1970), and that it should be about equal to the amplitude of (2). The sum of the two terms (i.e., curve C) then has the amplitude of  $15^{\circ}\text{K}$ . The annual mean of C is  $200^{\circ}\text{K}$ , a compromise between the values of CIRA and the U.S. Standard ( $205^{\circ}$  and  $185^{\circ}\text{K}$ , respectively). It is also readily apparent from curves A and C that incoherent

observations from the period April to October or absence of some monthly values could easily lead to the assumption of a single 12-mo variation with the maximum in winter as adopted in the U.S. Standard. But at least the amplitude given by the U.S. Standard may be roughly correct. If curve A represents true temperatures, its amplitude from October to December or December to April is about equal to the January–July amplitude of curve B.

Curve A in figure 10 is described very closely by the sum of (1) a semiannual term with the shape of J and the amplitude of  $24^{\circ}\text{K}$ , and (2) a sinusoidal 12-mo term with the maximum in July and the amplitude of  $30^{\circ}\text{K}$ . The phase of the 12-mo term would be opposite in the two hemispheres and its amplitude would increase with latitude. In the Northern Hemisphere, this phase reversal together with an invariant J term would still produce a two-peaked curve essentially similar to curve A (fig. 10) but with a larger amplitude. In reality, this asymmetry may be only a small one if the 12-mo terms in the two hemispheres are not an exact image of each other.

Another inference from figure 10 is that the amplitude of the semiannual variation grows with elevation from  $13^{\circ}\text{K}$  at 80 km to  $24^{\circ}\text{K}$  for the mean temperature of the 80- to 104-km layer and to  $128^{\circ}\text{K}$  in the middle thermosphere.

It must be stressed here that none of our estimates of temperature variations (figs. 10–14) was checked for generation of atmospheric structure that would conform to findings from satellite heights. The problem is not uniquely defined (Jacchia 1966) and would involve further assumptions about density variations not justified at present.

## 7. INFERRED VERTICAL TEMPERATURE PROFILES

With the technique discussed in the appendix, it was possible to reconstruct vertical temperature profiles. Examples for 6 mo of Adelaide data are shown by solid lines in figure 11. These profiles must be interpreted as being merely a gross approximation of actual conditions, indicative perhaps only of the sign of  $\Delta T/\Delta z$ . Plotted for comparison are two curves from the U.S. Standard for  $30^{\circ}$  latitude referring to January and July conditions in the Northern Hemisphere. The values of inferred temperatures agree reasonably well with those from the U.S. Standard, even near 104-km level. At 80 km, they are systematically higher, because an annual mean of  $200^{\circ}\text{K}$  was postulated for this level. Three curves in figure 11 show features that can be identified as the mesopause (M), with a sustained temperature increase above it. However, the curves for April and May suggest a puzzling temperature decrease in the lower thermosphere. In the thirteen months of Adelaide data, August (not shown) and, to a small degree, July, also have this characteristic. This suggests relatively low 104-km temperatures during the Southern Hemisphere winter, as if a seasonal term characterized by warm summer and cold winter was reappearing. A somewhat analogous modification of temperature profile in the vicinity of the tur-



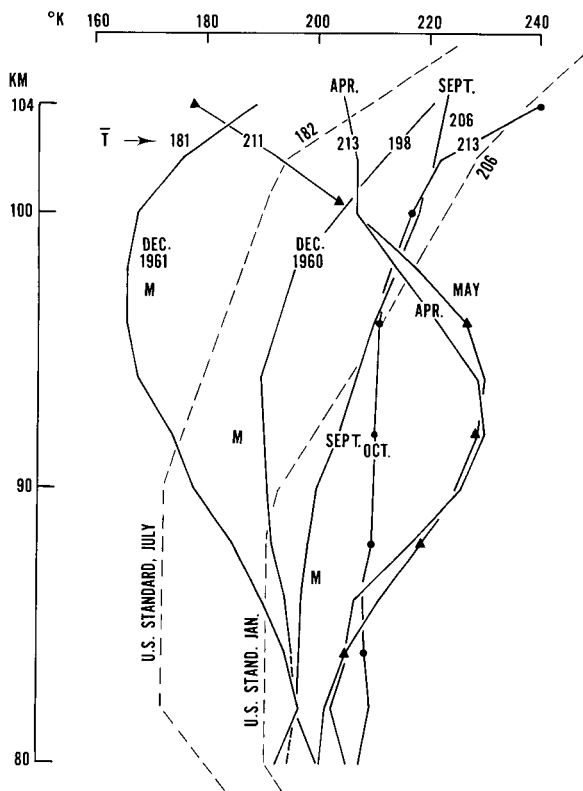


FIGURE 11.—Hypothetical monthly temperature profiles for Adelaide in 1961, compared with January and July profiles for the Northern Hemisphere from the U.S. Standard. The values of  $\bar{T}$  show mean temperatures of the 80- to 104-km layer. The letters M identify possible mesopauses.

bopause has been observed by Wand and Perkins (1968), who found a temperature maximum near 106 km and a minimum near 114 km with deviations from CIRA values being  $+80^\circ$  and  $-40^\circ\text{K}$ , respectively.

## 8. MODEL OF VARYING TEMPERATURE STRUCTURE

If temperature estimates for Adelaide are realistic, one should be able to explain their variability and connect them with shear observations. Systematic changes of the thermal structure within the 80- to 104-km layer may well be the direct cause. In examining this idea, it would be prudent not to depart from the temperature extremes and lapse rates of the U.S. Standard, as they are; after all, a fair estimate. According to this source, at  $30^\circ$  latitude an isothermal mesopause is located in the 80-90 km region while above it the temperature rises steeply and attains a lapse rate of  $14^\circ\text{K/km}$  at heights 112-120 km. Similar conditions prevail at  $60^\circ$  latitude. Even small departures from this structure at certain levels produce effects that are magnified with increasing elevation. Schilling (1968) has discussed this concept and shows how densities in the lower thermosphere may vary in response to changes in mesopause temperature and altitude.

For simplicity, we shall assume that, in the 80- to 104-km region, temperature changes may occur that are equivalent to displacing the U.S. Standard profiles up or down by 2 and 4 km. In the case of a downward shift, the

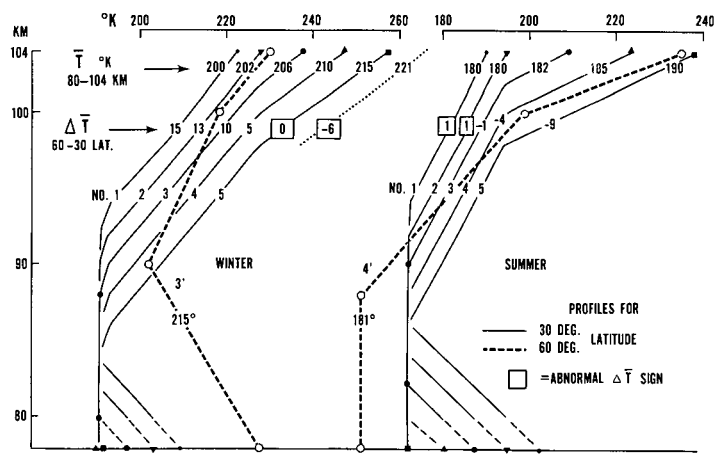


FIGURE 12.—A model illustrating possible temperature changes within the 80- to 104-km layer caused by vertical displacements of the basic temperature structure. Note changes in the mean temperature of this layer ( $\bar{T}$ ) and in the temperature differences between  $60^\circ$  and  $30^\circ$  latitude ( $\Delta\bar{T}$ ).

mean temperature of the 80- to 104-km layer will rise substantially because high temperatures of the lower thermosphere will appear below 104 km.

The results of such shifts are shown in figure 12, where solid lines refer to  $30^\circ$  latitude and dashed lines to  $60^\circ$  latitude. Curves 3 represent unaltered profiles from the U.S. Standard for  $30^\circ$  latitude; curves 2 and 1 correspond to upward displacement by 2 and 4 km, respectively; curves 4 and 5 to downward shifts by the same amounts. For  $60^\circ$  latitude, the shift is zero for curve 3' and 2 km downward for curve 4'. Indicated on each curve is the mean temperature of the 80- to 104-km layer ( $\bar{T}$ ), and the temperature difference between  $60^\circ$  and  $30^\circ$  latitude ( $\Delta\bar{T}$ ). It is seen that appreciable variations in  $\bar{T}$  result from the vertical shifts, but changes in  $\Delta\bar{T}$  are even more telling. In winter, the normal value of  $\Delta\bar{T}$  from the U.S. Standard is  $10^\circ\text{K}$ , implying a 31 m/s easterly shear that compares well with the 41 m/s average shear observed at Adelaide in the period May-September. In August 1961, the shear at Adelaide was nearly zero, and this would correspond in our winter array to curve 5. In some years, even a westerly shear may be expected in August, and such an abnormal situation could be caused by a 6-km downward shift of standard temperature profile at  $30^\circ$  latitude. The latter is shown by the dotted line with a  $\Delta\bar{T}$  value of  $-6^\circ\text{K}$ .

In summer, the normal  $\Delta\bar{T}$  value from the U.S. Standard is  $-6^\circ\text{K}$ , implying a westerly shear of 20 m/s. At Adelaide, the shear in December 1961 was westerly 65 m/s, but in the other 3 summer mo the shear was easterly about 8 m/s. In the model curves for summer (fig. 12), such abnormal easterly shears are represented by the boxed values of  $\Delta\bar{T}$ , while near-normal conditions are depicted by the values of  $-4^\circ$  and  $-9^\circ\text{K}$ .

Figure 12 shows only selected examples of shifts, but the model can be examined more generally by randomly combining profiles from latitudes  $30^\circ$  and  $60^\circ$ . The results indicate that in winter  $\bar{T}$  ( $60^\circ$  lat.)  $> \bar{T}$  ( $30^\circ$  lat.) in 92 percent of the cases, while in summer  $\bar{T}$  ( $60^\circ$  lat.)  $< \bar{T}$



(30° lat.) on 76 percent of the occasions. In the remaining cases, the sign of  $\Delta \bar{T}$  reverses; that is,  $\Delta \bar{T}$  is abnormal. Thus, the model is sufficient to explain shear variations at Adelaide and Birdlings Flat. The lifting and lowering of the mesopause and adjacent portions of the thermosphere could produce, not only changes in the mean temperature of the 80- to 104-km layer consistent with those previously shown in figure 10, but also variations in latitudinal gradient required by the observed shears. The range provided by the model is sufficient to account for the semi-annual effect and for the variability of monthly means in individual years.

The ultimate cause implied by the model would be abnormal heating or cooling near the turbopause. One notes that, for 4-km displacements, the model would require temperature departures of  $\pm 30^\circ\text{K}$  from the U.S. Standard at 104 km. For 120 km, rather large departures of  $\pm 50^\circ\text{K}$  could be expected. Cook (1969) has shown that such temperature variations at the 120-km boundary produce maximum effects near 200 km, with sharply decaying influence in the exosphere. Smaller variations are necessary if suitable density oscillations are assumed near 120 km.

## 9. LATITUDINAL VARIATION IN TEMPERATURE

From the inferred temperatures at Adelaide, temperature values at higher latitudes can be derived using the thermal wind relation. For estimates at 60° latitude, shears from Adelaide and Jodrell Bank were averaged. Because their shear magnitudes were in the ratio of 4 to 1, the averages were still weighted toward Adelaide data.

In figure 13, curve A represents temperature estimates for Adelaide while B shows derived values for 60° latitude. Of main interest is a comparison with temperatures obtained from the model discussed in section 8. These model temperatures are shown by four groups of horizontal lines valid for Southern Hemisphere winter and summer. Dashed horizontal lines are mean temperatures of the 80- to 104-km layer from the U.S. Standard, raised by 6°K to obtain a better fit. Solid horizontal lines depict means for profiles displaced vertically by 2 and 4 km. One sees that the horizontal lines account well for variations displayed by curves A and B. The equinoctial peaks shown by curve B have been noted, at least for lower levels, in observations. Quiroz (1969) indicated that the mean temperature of the 70- to 80-km layer at Churchill (59°N) has maxima in October (220°K) and April (208°K), with minima of about 186°K in July and at the end of February.

By using the same data as in figure 13 and extending our estimates to the pole, we obtain temperatures of 173°, 228°, 231°, and 238°K for December, April, June, and October, respectively. An extrapolation of the U.S. Standard values gives 170°K for summer and 222°K for winter, rendering perhaps only our October estimate as excessively high. For Heiss Island (81°N), Quiroz found the 80-km temperatures changing from 245°K in late September to 189°K in late October. One of the conclusions from figure 13 is, however, that the strong

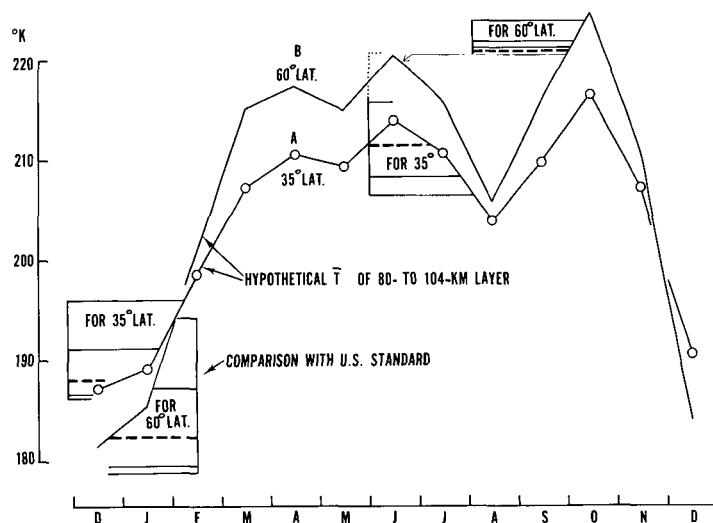


FIGURE 13.—Hypothetical mean temperatures of the 80- to 104-km layer at Adelaide (curve A) and at 60° latitude (curve B). The latter was derived from the thermal wind relation by using A and averaged shears from Jodrell Bank and Adelaide. Four groups of horizontal lines show peak summer and winter values suggested by the U.S. Standard and by model temperature changes from figure 12.

horizontal temperature gradient near 35°S indicated by Adelaide 1961 shears must slacken considerably at higher latitudes. Such a slackening has been suggested earlier (Kochanski 1963) by different data series from Adelaide.

## 10. DISTRIBUTION OF TEMPERATURE OSCILLATIONS

The range of the semiannual,  $R_6$ , and annual temperature,  $R_{12}$ , variation may have a distribution shown as in figure 14. This is a composite picture that utilizes data from Angell and Korshover (1970) for the A region and values from the U.S. Standard for the 12-mo variation in the B region. Solid lines refer to the semiannual variation, dashed ones to the 12-mo term. Dotted lines delineate areas with a dominant 6-mo term. In A region, below line P, the maximum of the 12-mo variation is in summer whereas in the B region it occurs in winter. For the C region above line P', the U.S. Standard postulates yet another seasonal variation with the maximum in summer. This concept has some weak support from the topmost data at Adelaide.

A purely hypothetical feature in figure 14 is the vertical distribution of  $R_6$  values from 90 km upward. We assumed a constant gradient of  $10^\circ\text{K}/14.3 \text{ km}$  for  $R_6$ , which would give a range of  $100^\circ\text{K}$  at the height of 200 km. An identical value has been obtained by Jacchia et al. (1969) for the 1958-66 semiannual variation of exospheric temperatures normalized to flux  $\bar{F}_{10.7 \text{ cm}} = 100 \times 10^{-22} \text{ W} \cdot \text{m}^{-2} \cdot \text{c} \cdot \text{s}^{-1}$ . Figure 14 also suggests that if the correlation between the variations of shear and temperature holds, a purely semiannual shear oscillation should appear along line P'. This is the case for Jodrell Bank and Kühlungsborn shears, providing line P' lies at somewhat lower heights than shown in figure 14. Quantitatively, some features in

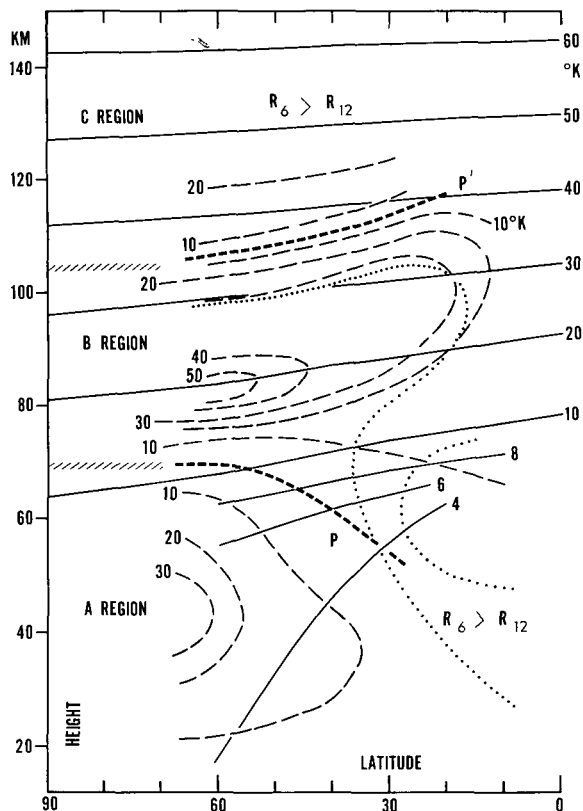


FIGURE 14.—Possible distribution of the range of semiannual (solid lines) and annual (dashed lines) temperature variation. Lines P and P' delineate zones of phase reversal of the 12-mo variation. Data to 61 km are from Angell and Korshover (1970) and values of the 12-mo variation in the B region are from the U.S. Standard.

figure 14 are of course questionable (e.g., 50°K line in  $R_{12}$ ) but they do not change the basic pattern. An apparent discrepancy concerning a weak semiannual shear variation at 53°N and a strong one at 35°S may be due simply to changeable correlation between shear and temperature. At various latitudes a different conversion factor must apply, as is evident from the construction of that factor (see appendix).

## 11. VARIATIONS IN TIDAL MOTIONS AND ENERGY EXCHANGE

There is some evidence of the semiannual variation in both the tidal motions and the energy dissipation rates at meteor heights. At Adelaide, this may be simply a function of the double passage of the sun, but the effect is also present in tidal parameters at Jodrell Bank.

Examples are given in figure 15, where J represents exospheric temperature variations in 1961, and other lines are based on Adelaide data for 1961. Curves A24, A12, and A8 depict tidal amplitudes for the 24-, 12-, and 8-hr tides, respectively, and represent averages for the 83- to 99-km layer where the errors of estimate were minimum; shown are total amplitudes  $|A| = (A_u^2 + A_v^2)^{1/2}$ . Curve  $|V|$  illustrates the magnitude of the prevailing wind vector. Curve  $\epsilon$  depicts the rate of dissipation of turbulent energy, taken from Roper and Elford (1963). In all these curves, there are traces of the semiannual effect in the form of major or

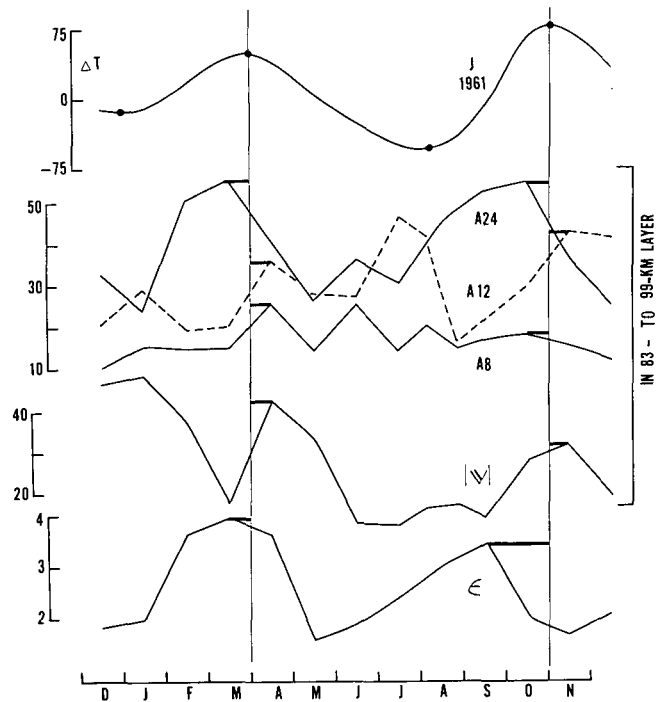


FIGURE 15.—Traces of the semiannual effect in parameters of motion at Adelaide. Curves A24, A12, and A8 refer to tidal amplitudes (m/s),  $|V|$  is the scalar speed of the prevailing wind (m/s), and  $\epsilon$  is the rate of dissipation of turbulent energy ( $10^{-2}$  W/kg). Curve J represents semiannual variation of exospheric temperatures (°K) in 1961.

minor peaks near April and October; the same applies to minimum values around January and July or August. A fair overall similarity to J is shown by curve A24. In curve  $\epsilon$  most features, except the April maximum, are out of phase with J. However, the values of  $\epsilon$  account only for eddies up to 3 km in diameter and this may be a partial explanation of their nonconforming pattern. Other curves, especially A8 and A12, exhibit noiselike irregularities that may stem from the reduction technique that employed tidal Fourier series in time and least-square polynomials in the vertical.

If the rather weak evidence from figure 15 is correct, it may indicate that at meteor heights the semiannual variation is a basic phenomenon that extends to tidal motions and energy exchange mechanisms.

## 12. SUMMARY

One can surmise that a complex interweaving of semiannual, annual, and latitudinal effects takes place in the lower thermosphere. The behavior of the temperature is a matter of conjecture, but we can speak with some certainty about the parameters of motion. The semiannual effect in the zonal component of the prevailing wind and its shears is seen within 35°–55° latitude at 80- to 105-km heights, but superimposed on it near 35° latitude there is a 12-mo term; it is likely that this term appears in a layer that slopes downward in high latitudes, below meteor heights. Similar variations must exist in the latitudinal temperature gradient, which is a function of shears. Some information from greater altitudes can be

obtained by considering a "prevailing wind" isolated from sodium cloud drifts near 35°N (Kochanski 1966), with the reservation that it represents only twilight conditions. In the 90- to 110-km region, the zonal component of this wind has an easterly shear of 40 m/s, being identical to the 80- to 105-km shear from Adelaide meteor data. Within 110- to 160-km heights, this zonal component shows no significant summer-winter differences and amounts to 20-45 m/s. Because the effect of the ion drag is not dominant below 160 km, such a zonal wind can be maintained only by latitudinally organized thermal systems; coexisting with this latitudinal effect there may be a semiannual variation in shears and horizontal temperature gradient. In all these cases, the semiannual effect is in phase with similar variation of density at heights greater than 200 km.

With regard to temperature, the U.S. Standard terminates latitudinal variations at 120 km but assumes that summer-winter changes exist up to 250 km. CIRA postulates a model in which seasonal and latitudinal variations vanish within the 100- to 120-km layer. Neither CIRA nor the U.S. Standard stipulates a semiannual effect near the base of the thermosphere. Our supposition is, however, that an appreciable 6-mo term is present in the 80- to 105-km layer apart from seasonal and latitudinal changes. It may well be that the last two effects attenuate with elevation, exposing, at some heights not far removed from 120 km, a semiannual variation as the third main factor in addition to diurnal and solar cycle changes.

The problem of a plausible physical explanation for the semiannual variation in the thermosphere still remains. One possibility is that the upper atmosphere merely responds to changes occurring in the stratosphere, where the solar ultraviolet heat input is concentrated. Significant amounts of energy enter the upper atmosphere through dynamical coupling from the lower atmosphere, but the mechanisms of such a transfer are at present uncertain. Webb (1966) pointed out that hydrostatic changes observed in the mesosphere seem to be simply a compensation for stratospheric changes, and that stratospheric warm anticyclonic vortexes appearing at the poles around equinoxes could grow with elevation. However, the nature of such an amplification with height and equatorward spreading is unclear, considering that it must lead to a semiannual variation that is uniform for all latitudes and at all heights within at least the 200- to 1100-km range. Cook (1969) suggested that the source of the semiannual effect is likely to be within the 80- to 200-km region or possibly even in lower strata.

## APPENDIX

### Thermal Wind Equation and Its Transform

The full thermal wind equation (Brunt 1934) was too detailed to be used in present considerations. The approximate thermal wind equation, valid for an isothermal atmosphere and geostrophic zonal flow, is usually written as

$$\frac{\partial T}{\partial y} = -\frac{f}{g} T \frac{\partial u}{\partial z} \quad (1)$$

where  $\partial u/\partial z$  is vertical shear of the zonal wind,  $T$  is the mean temperature of the layer at the site of  $\partial u/\partial z$  and  $\partial T/\partial y$  is latitudinal temperature gradient in the poleward direction. Decreasing westerlies or increasing easterlies indicate warmer air toward the pole. Constants  $f$  and  $g$  are the Coriolis parameter and acceleration due to gravity, respectively.

For the particular case of the 80- to 105-km layer, it is proposed to restrict eq (1) to a specific relationship between  $T$  and shears, based on evidence from Adelaide and Jodrell Bank data. By using the directional locations of warm and cold centers and the mean 79- to 105-km wind, advective temperature changes were established. In a substantial majority of cases, the easterly shear was highly correlated with warm advection while the westerly shear corresponded to cold advection. For the 13 monthly means of Adelaide data, this relation was clearly confirmed in nine cases, clearly contradicted in one case, while the remaining three cases were marginal but could confirm the relation if a slight change of the layer depth were made. For Jodrell Bank, eight cases were confirmatory and four marginal. This suggests that the mean temperature of the 80- to 105-km layer is higher than the 80-km temperature in case of an easterly shear and lower for a westerly shear.

In addition, it is assumed that changes of temperature with elevation are proportional to changes in integrated shear. Consider layers of increasing thickness composed of thin strata for which shear values,  $\partial u/\partial z$ , are known. These layers have a common lower boundary having temperature  $T_0$ . It is postulated that

$$T_i - T_0 \propto \sum_i^n (\partial u/\partial z) \quad (2)$$

or

$$T_i \propto T_0 + dT$$

where  $T_i$  represents mean temperature of a layer and  $dT$  is a temperature increment in the vertical. The summation is for  $i = 1, 2, \dots, n$  where  $i$  is the number of the stratum. It then remains to find a scale factor between shear and  $dT$  such that it would not violate basic eq (1). In the finite form, eq (1) becomes

$$c\Delta u = \Delta T/T \quad (3)$$

where  $\Delta z$  and  $\Delta y$  are incorporated in  $c$ . Substitution from eq (2) yields

$$c\Delta u = \Delta T/(T_0 + dT) \quad (4)$$

or

$$c\Delta u/T = \Delta T/(TT_0 + TdT). \quad (5)$$

The U.S. Standard suggests that at all latitudes between 30° and 60° the mean annual  $T$  of the 80- to 105-km layer is close to 195°K and  $dT$  is about 7°K. Hence, in eq (5) the term  $TdT$  is very small in comparison with  $TT_0$  and can be neglected; also,  $TT_0 \approx T^2$ . Furthermore, from eq (1) and (2) the transform  $dT \equiv \Delta T$  is assumed valid. Then

$$\Delta u/T = \Delta T/cT^2 \quad (6)$$

or

$$\Delta u/T = dT/cT^2. \quad (7)$$

The scale factor is found by setting  $\Delta T = 1^\circ\text{K}$  and then  $\Delta u = 1$  m/s. Because latitudinal gradients are involved, further considerations are restricted to Adelaide. If we give equal weight to the U.S. Standard  $\Delta T$  value between  $30^\circ$  and  $60^\circ$  latitude ( $7.5^\circ\text{K}$ ) and to average shear magnitude from Adelaide [ $40 \text{ m}\cdot\text{s}^{-1}\cdot(26 \text{ km})^{-1}$ ], we find  $\Delta T/\Delta y = 1^\circ\text{K}/385 \text{ km}$ . Then from eq (1) constant  $c = 1.6 \times 10^{-4}$  s/m. Letting  $\Delta u = 1$  m/s and  $T = 200^\circ\text{K}$  in eq (1), we obtain  $\Delta T = 0.032^\circ\text{K}$ . This value and  $\Delta u = 1$  m/s satisfy eq (7) for  $cT^2 = 6.4(^\circ\text{K})^2\cdot\text{s}\cdot\text{m}^{-1}$ , where  $cT^2$  is the scale factor between  $\Delta u$  and  $dT$  and varies from 5.18 for  $T = 180^\circ\text{K}$  to 7.74 for  $T = 220^\circ\text{K}$ . For actual conversion, eq (7) reduces to  $dT = \Delta u/cT^2$ .

Computed  $dT$  values must satisfy eq (1) in the sense that the magnitude of  $\Delta y$  should be reasonable. The average  $dT$  from Adelaide shears was  $6^\circ\text{K}$ , yielding a  $\Delta y$  of  $20^\circ$  latitude, a somewhat large but not unlikely distance over which the assumptions were valid; especially for broad-scale thermal systems that presumably exist at the heights under consideration.

The conversion of a monthly shear value consisted of assuming a certain temperature,  $T_0$ , at the bottom of the shear profile (i.e., at 80 km) and finding  $T_2$  (i.e., the mean temperature of the 80- to 105-km layer). As the first estimate,  $T_1$  was computed where

$$T_1 = T_0 + \Delta u/cT_0^2. \quad (8)$$

The second estimate was obtained from

$$T_2 = T_0 + 2\Delta u/(cT_0^2 + cT_1^2) \quad (9)$$

where  $T_2$  was the accepted value. Temperatures shown in figure 10 were derived from eq (9). To obtain vertical temperature profiles, a linear scale was assumed between  $T_0$  and  $T_2$  on curves of integrated shear, and temperatures of progressively thicker layers were read off. From these values, mean temperatures of 2-km layers were computed using

$$T_{2 \text{ km}} = T_n(n) - T_{n-1}(n-1) \quad (10)$$

where  $T_n$  and  $T_{n-1}$  are temperatures of two adjacent layers, while  $n$  and  $n-1$  are the number of 2-km strata in these layers. The inferred temperature profiles are shown in figure 11.

*Note added in proof*—Recently, Jacchia (1971) has radically reappraised the premise that the semiannual density variation is caused by a parallel temperature variation in the heterosphere. Apparently, the semiannual effect in temperature may be minimal or at least considerably smaller than previously thought. An interaction between solar wind and the magnetosphere may be involved as a cause of the observed density variation, but no firm theory is yet available. The question remains whether this applies to the base of the thermosphere where a propagation of semiannual temperature effect from the mesosphere may occur. Also, the appearance of a dominant semiannual variation in a surprisingly large number of atmospheric parameters will have to be explained.

## ACKNOWLEDGMENTS

The author is indebted to G. J. Fraser, University of Canterbury, New Zealand, for permission to use his unpublished data on ionospheric drifts from Birdlings Flat. Many thanks are also due G. F. Cotton and T. H. Carpenter of NOAA Air Resources Laboratories for their valuable suggestions and their help in computerizing some of the analyses.

## REFERENCES

- Angell, J. K., and Korshover, J., "Quasi-Biennial, Annual, and Semiannual Zonal Wind and Temperature Harmonic Amplitudes and Phases in the Stratosphere and Low Mesosphere of the Northern Hemisphere." *Journal of Geophysical Research, Oceans and Atmospheres*, Vol. 75, No. 3, Jan. 20, 1970, pp. 543-550.
- Becker, Walter, "The Seasonal Anomaly of the F Region at Mid-Latitudes and Its Interpretation," *Electron Density Profiles in Ionosphere and Exosphere*, North-Holland Publishing Co., Amsterdam, The Netherlands, 1966, pp. 218-230.
- Brunt, David, *Physical and Dynamical Meteorology*, Cambridge University Press, London, England, 1934, 411 pp.
- COESA, U.S. Committee on Extension to the Standard Atmosphere, *U.S. Standard Atmosphere Supplements, 1966*, U.S. Government Printing Office, Washington, D.C., 1966, 289 pp.
- Cole, Allen E., "Periodic Oscillations in the Tropical and Subtropical Atmosphere at Levels Between 25 and 80 Km," *Space Research*, Vol. 8, North-Holland Publishing Co., Amsterdam, The Netherlands, 1968, pp. 823-834.
- Cook, G. E., "The Large Semi-Annual Variation in Exospheric Density: A Possible Explanation," *Planetary and Space Science*, Vol. 15, No. 4, Oxford, England, Apr. 1967, pp. 627-632.
- Cook, G. E., "Variations in Air Density at Heights Near 500 Km From 1965 to 1967," *Planetary and Space Science*, Vol. 16, No. 9, Oxford, England, Sept. 1968, pp. 1161-1176.
- Cook, G. E., "The Semi-Annual Variation in the Upper Atmosphere: A Review," *Annales de Géophysique*, Vol. 25, No. 2, Paris, France, Apr. 1969, pp. 451-469.
- Cook, G. E., and Scott, Diana W., "Exospheric Densities Near Solar Minimum Derived From the Orbit of Echo 2," *Planetary and Space Science*, Vol. 14, No. 11, Oxford, England, Nov. 1966, pp. 1149-1165.
- COSPAR Working Group IV, *COSPAR International Reference Atmosphere, 1965*, CIRA (1965), Committee on Space Research, North-Holland Publishing Co., Amsterdam, The Netherlands, 1965, 313 pp.
- Elford, W. G., and Roper, R. G., "Turbulence in the Lower Thermosphere," *Space Research*, Vol. 7, North-Holland Publishing Co., Amsterdam, The Netherlands, 1967, pp. 42-54.
- Fraser, G. J., and Kochanski, Adam, "Ionospheric Drifts From 64-108 Km Altitudes at Birdlings Flat," *Annales de Géophysique*, Vol. 26, No. 3, Paris, France, July/Sept. 1970, pp. 675-687.
- Greenhow, J. S., and Neufeld, E. L., "Winds in the Upper Atmosphere," *Quarterly Journal of the Royal Meteorological Society*, Vol. 87, No. 374, London, England, Oct. 1961, pp. 472-489.
- Groves, G. V., "A Theory for Determining Upper-Atmosphere Winds From Radio Observations on Meteor Trails," *Journal of Atmospheric and Terrestrial Physics*, Vol. 16, No. 3/4, Nov. 1959, pp. 344-356.
- Jacchia, Luigi G., "The Temperature Above the Thermopause," *Space Research*, Vol. 5, North-Holland Publishing Co., Amsterdam, The Netherlands, 1965, pp. 1152-1174.
- Jacchia, Luigi G., "Density Variations in the Heterosphere," *Annales de Géophysique*, Vol. 22, No. 1, Paris, France, Jan./Mar. 1966, pp. 75-85.
- Jacchia, Luigi G., "Semiannual Variation in the Heterosphere: A Reappraisal," *Journal of Geophysical Research, Space Physics*, Vol. 76, No. 19, July 1, 1971, pp. 4602-4607.

- Jacchia, Luigi G., Slowey, J. W., and Campbell, I. G., "A Study of the Semi-Annual Density Variation in the Upper Atmosphere From 1958 to 1966 Based on Satellite Drag Analysis," *Planetary and Space Science*, Vol. 17, No. 1, Oxford, England, Jan. 1969, pp. 49-60.
- Johnson, F. S., "Circulation at Ionospheric Levels," *Report*, Contract No. Cwb 10531, Southwest Center for Advanced Studies, Dallas, Tex., 1964, 24 pp.
- Kellogg, W. W., "Chemical Heating Above the Polar Mesopause in Winter," *Journal of Meteorology*, Vol. 18, No. 3, June 1961, pp. 373-381.
- King-Hele, D. G., and Hingston, Janice, "Air Density at Heights Near 190 Km in 1966-67, From the Orbit of Secor 6," *Planetary and Space Science*, Vol. 16, No. 5, Oxford, England, May 1968, pp. 675-691.
- Kochanski, Adam, "Circulation and Temperatures at 70- to 100-Kilometer Height," *Journal of Geophysical Research*, Vol. 68, No. 1, Jan. 1, 1963, pp. 213-226.
- Kochanski, Adam, "Atmospheric Motions From Sodium Cloud Drifts at Four Locations," *Monthly Weather Review*, Vol. 94, No. 4, Apr. 1966, pp. 199-212.
- Paetzold, Hans Karl, and Zschörner, H., "Bearings of Sputnik III and the Variable Acceleration of Satellites," *Space Research*, Vol. 1, North-Holland Publishing Co., Amsterdam, The Netherlands, 1960, pp. 24-36.
- Paetzold, Hans Karl, and Zschörner, H., "The Structure of the Upper Atmosphere and Its Variations After Satellite Observations," *Space Research*, Vol. 2, North-Holland Publishing Co., Amsterdam, The Netherlands, 1961, pp. 958-973.
- Quiroz, Roderick S., "The Warming of the Upper Stratosphere in February 1966 and the Associated Structure of the Mesosphere," *Monthly Weather Review*, Vol. 97, No. 8, Aug. 1969, pp. 541-552.
- Reed, Richard J., "Zonal Wind Behavior in the Equatorial Stratosphere and Lower Mesosphere," *Journal of Geophysical Research*, Vol. 71, No. 18, Sept. 15, 1966, pp. 4223-4233.
- Roper, R. G., and Elford, W. G., "Seasonal Variation of Turbulence in the Upper Atmosphere," *Nature*, Vol. 197, No. 4871, London, England, Mar. 9, 1963, pp. 963-964.
- Roper, R. G., and Elford, W. G., "Meteor Winds Measured at Adelaide (35°S) 1961," *NASA Technical Memorandum No. TM-X-55302*, U.S. National Aeronautics and Space Administration, Greenbelt, Md., June 1965, 166 pp.
- Schilling, Gerhard F., "Density and Temperature Variations in the Intervening Layer (90-150 Km)," *Meteorological Monographs*, Vol. 9, No. 31, American Meteorological Society, Boston, Mass., Apr. 1968, pp. 82-89.
- Sprenger, K., and Schminder, R., "Evidence of a 26-Month Wind Oscillation in the Lower Ionosphere Over Central Europe," *Zeitschrift für Meteorologie*, Vol. 19, No. 5/6, Berlin, West Germany, 1967, pp. 168-170.
- Sullivan, H. M., and Roberts, M. G., "Height of the Twilight Sodium Layer: Evening-Morning Effect Observed at Victoria, British Columbia From Feb. 1967 to Feb. 1968," *Nature*, Vol. 220, No. 5165, London, England, Oct. 26, 1968, pp. 361-362.
- Wand, R. H., and Perkins, F. W., "Radar Thomson Scatter Observations of Temperature and Ion-Neutral Collision Frequency in the E Region," *Journal of Geophysical Research, Space Physics*, Vol. 73, No. 19, Oct. 1, 1968, pp. 6370-6372.
- Warnecke, Günter, and Nordberg, W., "Inferences of Stratospheric and Mesospheric Circulation Systems From Rocket Experiments," *Space Research*, Vol. 5, North-Holland Publishing Co., Amsterdam, The Netherlands, 1965, pp. 1026-1038.
- Webb, Willis L., *Structure of the Stratosphere and Mesosphere*, Academic Press, New York, N.Y., 1966, 382 pp.

[Received June 26, 1970; revised October 22, 1970]